und Halbach-Stiftung, and the Deutsche Forschungsgemeinschaft is gratefully acknowledged.

Registry No. **7d**, 143733-05-5; **7e**, 143733-06-6; **11a**, 105253-58-5; **11b**, 113177-54-1; **12**, 105102-80-5; **14a**, 143733-02-2; **14b**, 143733-03-3; **14c**, 143733-04-4; **15**, 143733-07-7; $AlMe_3$, 75-24-1; $AlEt_3$, 97-93-8; BEt_3, 97-94-9.

Supplementary Material Available: Tables listing details of the X-ray structure analyses of **14a** and **14b** and complete listings of bond lengths and angles (18 pages). Ordering information is given on any current masthead page.

OM920215K

Regioselective Hydroformylation of Cyclic Vinyl and Allyl Ethers with Rhodium Catalysts. Crucial Influence of the Size of the Phosphorus Cocatalyst

Alfonso Polo, Carmen Claver,* Sergio Castillón,* and Aurora Ruiz

Departament de Química, Facultat de Ciències Químiques de Tarragona, Universitat de Barcelona, Pça Imperial Tarraco 1, 43005 Tarragona, Spain

Juan Carlos Bayón* and Julio Real

Departament de Química, Universitat Autònoma de Barcelona, 08193 Bellaterra, Barcelona, Spain

Carlo Mealli and Dante Masi

Istituto per lo Studio della Stereochimica ed Energetica dei Composti di Coordinazione, Via J. Nardi 39, 50132 Firenze, Italy

Received February 21, 1992

In the course of studies aimed at developing new catalytic systems, we have explored the possibilities offered by the modification of thiolato bridges in dinuclear rhodium complexes, together with the influence of the cocatalyst, on the selective hydroformylation of cyclic vinyl and allyl ethers. The dinuclear complex $[Rh_2(\mu\text{-}S(CH_2)_3NMe_2)_2(cod)_2]$ (cod = 1,5-cyclooctadiene) has been prepared, and its reactivity with CO, phosphines, and phosphites has been investigated. The complex crystallizes in the monoclinic space group $C2/c$ with $Z = 8$, $a = 22.543$ (4) Å, $b = 12.040$ (2) Å, $c = 21.547$ (3) Å, and $\beta = 98.77$ (1)°. For the determination of the structure 4091 unique reflections were used, and the final refinement gave $R = 4.1\%$ and $R_w = 4.4\%$. The molecular structure reveals that the two rhodium atoms are bridged by the two thiolato ligands, and the cyclooctadiene completes the coordination of the metal atoms. The amine groups are not bonded to the rhodium. The dinuclear complex has been used in the hydroformylation of 2,3-dihydrofuran, 2,5-dihydrofuran, 3,4-dihydro-2*H*-pyran, and 3,6-dihydro-2*H*-pyran. Hydroformylation reactions of dihydrofurans required conditions milder than those for dihydropyrans. The major product in the hydroformylation of 3,4-dihydro-2*H*-pyran or 3,6-dihydro-2*H*-pyran was tetrahydropyran-2-carbaldehyde. A systematic study of the influence of the reaction parameters on the selectivity of the hydroformylation of 2,3-dihydrofuran and 2,5-dihydrofuran was undertaken. The study allowed the rationalization of the observed selectivity and the optimization of the yields and regioselectivities. Thus, by modification of the reaction parameters, tetrahydrofuran-3-carbaldehyde was obtained in quantitative yields from 2,5-dihydrofuran and tetrahydrofuran-2-carbaldehyde can be prepared from either 2,3-dihydrofuran or 2,5-dihydrofuran in approximately 75% yield.

Introduction

The hydroformylation of propene is one of the few processes in which homogeneous catalysts are employed on a large industrial scale.[1] Although the reaction has been known for many years, much work has recently been devoted to the preparation of new, active, highly selective catalytic systems,[2,3] the recovery of the catalyst,[4] the study of the reaction mechanism,[5] and the use of the process in the synthesis of fine chemicals.[6] With regard to this last point, the hydroformylation of functionalized alkenes has recently been reviewed.[7] The reactions of cyclic functionalized alkenes are a special case. The hydroformylation of some of these substrates yields aldehydes which are of interest for the preparation of intermediates for the synthesis of natural products or pharmaceuticals.[8] However,

(1) (a) Cornils, B. In *New Synthesis with Carbon Monoxide*; Falbe, J., Ed.; Springer-Verlag: Berlin, 1980; pp 1–225. (b) Pruett, R. L. *Adv. Organomet. Chem.* **1979**, *17*, 1–60. (c) Tkatchenko, I. In *Comprehensive Organometallic Chemistry*; Wilkinson, G., Ed.; Pergamon Press: Oxford, U.K., 1982; Vol. 8, pp 101–223. (d) Botteghi, C.; Gladialli, S.; Bellagamba, V.; Ercoli, R.; Gamba, A. *Chim. Ind.* **1980**, *62*, 604. (e) **1981**, *63*, 29. (f) Pino, P. *J. Organomet. Chem.* **1980**, *200*, 223.

(2) McDougall, J. K.; Cole-Hamilton, D. J. *J. Chem. Soc., Chem. Commun.* **1990**, 165.

(3) (a) Bergounhou, C.; Neibecker, D.; Reau, P. *J. Chem. Soc., Chem. Commun.* **1988**, 1370. (b) Neibecker, D.; Reau, P. *Angew. Chem., Int. Ed. Engl.* **1989**, 500. (c) Neibecker, D.; Reau, P. *J. Mol. Catal.* **1989**, *53*, 219.

(4) Terreros, P.; Pastor, E.; Fierro, J. L. G. *J. Mol. Catal.* **1989**, 359.

(5) Lazzaroni, R.; Pertici, P.; Bertozzi, S.; Fabrizi, G. *J. Mol. Catal.* **1990**, *58*, 75 and references cited therein.

(6) (a) Burke, S. D.; Cobb, J. E.; Takeniche, K. *J. Org. Chem.* **1990**, *55*, 2138. (b) Doyle, M. M.; Jackson, W. R.; Perlmutter, P. *Tetrahedron Lett.* **1989**, *30*, 233. (c) Kollar, L.; Bakos, J.; Heil, B.; Jardor, P.; Szalontai, G. *J. Organomet. Chem.* **1990**, *385*, 147.

(7) Botteghi, C.; Ganzerla, R.; Lenarda, M.; Moretti, G. *J. Mol. Catal.* **1987**, *40*, 129.

(8) Siegel, H.; Himmele, W. *Angew. Chem., Int. Ed. Engl.* **1980**, *19*, 178.

0276-7333/92/2311-3525$03.00/0

there have been few reports of the successful hydroformylation of internal cyclic alkenes. In most cases, drastic reaction conditions are required and, probably for that reason, only moderate selectivities may be achieved.[9] In recent years, the use of bulky phosphites in rhodium–phosphorus catalytic systems has been found to be useful in the hydroformylation of cycloalkenes.[10]

In 1983, Kalck reported a new type of dinuclear rhodium thiolato complexes as catalysts for alkene hydroformylation.[11] There have since been other reports of the use of related dinuclear complexes, some of these showing excellent activity, under mild conditions, for 1-hexene hydroformylation.[12]

In the course of studies aimed at the development of new catalytic systems, via modification of the thiolato bridges in the dinuclear rhodium complexes, we have recently reported the use of $[Rh_2(\mu\text{-}S(CH_2)_3NMe_2)_2(cod)_2]$ (cod = 1,5-cyclooctadiene) as a selective catalyst precursor for the hydroformylation of 1-hexene. This catalyst was shown to be very active under mild conditions (5 bar and 80 °C).[13] Thus, it was of interest to study its activity in the hydroformylation of a range of dihydrofurans and dihydropyrans. The aim of this work is to determine the factors controlling the regioselectivity in the hydroformylation of cyclic vinyl and allyl ethers, as a model for the functionalization of unsaturated furanoside and pyranoside natural products. In the hydroformylation of linear vinyl ethers high regioselectivities in the branched aldehyde have been achieved. However, no general trends are observed in the product distributions for the hydroformylation of linear allylic ethers, the selectivity being highly dependent on the reaction conditions and the nature of the catalyst.[14] On the other hand, only two previous reports deal with the hydroformylation of dihydrofurans catalyzed by rhodium catalysts. In both cases high pressures were used, and the selectivity toward tetrahydrofuran-2-carbaldehyde observed was low.[15] The hydroformylation of dihydropyrans catalyzed by a cobalt catalyst has also been reported.[16] In that case, very drastic conditions were required, and 2-(hydroxymethyl)tetrahydropyran was the major reaction product. The hydrocarbonylation of cyclic vinyl- and allylamines has been very recently reported. The results show that the 2-derivative, acid or aldehyde, is the major reaction product.[17]

We report here a complete study of the regioselective hydroformylation of dihydrofurans and dihydropyrans, together with a model for the mechanism based on the selectivity of the reaction, and studies toward determining the nature of the active catalytic species. The structure of the dinuclear catalyst precursor has been established by X-ray crystallography.

Table I. Atomic Coordinates for the Structure of $[Rh_2(\mu\text{-}S(CH_2)_3NMe_2)_2(cod)_2]$ (Values Multiplied by 10^4)[a]

atom	x	y	z
Rh1	1171 (0.2)	2759 (0.4)	1035 (0.3)
Rh2	1310 (0.2)	378 (0.4)	1365 (0.2)
S1	595 (1)	1234 (1)	615 (1)
S2	1879 (1)	1483 (2)	782 (1)
C1	−186 (3)	1150 (5)	732 (3)
C2	−589 (3)	1728 (6)	203 (3)
C6	2661 (3)	1740 (8)	1127 (5)
C7	3074 (3)	1231 (10)	722 (6)
C11	514 (3)	3514 (8)	1504 (5)
C12	1762 (3)	3673 (9)	1712 (5)
C13	497 (4)	4013 (7)	944 (5)
C14	1744 (4)	4166 (7)	1133 (6)
C15	797 (4)	3968 (12)	2131 (5)
C16	1442 (4)	4143 (12)	2215 (5)
C17	767 (5)	5164 (7)	850 (8)
C18	1412 (5)	5217 (8)	918 (7)
C19	1966 (4)	147 (7)	2186 (4)
C20	711 (3)	−19 (8)	2011 (4)
C21	2010 (3)	−711 (7)	1767 (4)
C22	772 (3)	−931 (6)	1639 (4)
C23	1685 (5)	7 (11)	2770 (4)
C24	1019 (5)	125 (11)	2677 (5)
C25	1778 (5)	−1873 (7)	1824 (6)
C26	1135 (4)	−1960 (8)	1844 (7)
N1	−1480 (3)	1687 (6)	744 (3)
N2	3963 (3)	1989 (7)	1364 (3)
C3	−1250 (4)	1456 (8)	165 (4)
C4	−2100 (5)	1259 (13)	684 (7)
C5	−1442 (7)	2881 (10)	890 (8)
C8	3718 (6)	972 (11)	1104 (8)
C9	4543 (6)	1847 (14)	1788 (7)
C10	4052 (8)	2869 (13)	916 (8)
C3″	−1145 (10)	2340 (18)	354 (14)
C4″	−1858 (15)	787 (24)	425 (17)
C5″	−1972 (13)	2211 (32)	1018 (17)
C8″	3696 (8)	1745 (24)	706 (8)
C9″	4081 (20)	874 (20)	1631 (21)
C10″	4547 (10)	2513 (29)	1360 (18)

[a] Carbons marked with a double prime constitute, with the corresponding unprimed atom, a double image of the atoms linked to the nitrogens. The disorder is accounted for by pairs of population parameters refined to 0.7 and 0.3 for unprimed and primed atoms, respectively.

Table II. Selected Distances (Å) and Angles (deg) for $[Rh_2(\mu\text{-}S(CH_2)_3NMe_2)_2(cod)_2]$

Rh1–S1	2.349 (2)	Rh2–C20	2.137 (9)
Rh1–S2	2.339 (2)	Rh2–C21	2.132 (7)
Rh2–S1	2.341 (1)	Rh2–C22	2.127 (8)
Rh2–S2	2.343 (2)	C11–C13	1.34 (2)
Rh1–C11	2.12 (1)	C12–C14	1.38 (2)
Rh1–C12	2.13 (1)	C19–C21	1.39 (1)
Rh1–C13	2.128 (8)	C20–C22	1.38 (1)
Rh1–C14	2.122 (9)	Rh1···Rh2	2.960 (1)
Rh2–C19	2.145 (8)		
Rh1–S1–Rh2	78.3 (1)	S2–Rh1–C11	160.6 (3)
Rh1–S2–Rh2	78.4 (1)	S2–Rh1–C12	97.0 (2)
S1–Rh1–S2	75.7 (1)	S2–Rh1–C13	161.2 (3)
S1–Rh2–S2	75.8 (1)	S2–Rh1–C14	96.9 (3)
Rh1–S1–C1	118.6 (2)	S1–Rh2–C19	160.5 (2)
Rh2–S1–C1	117.3 (2)	S1–Rh2–C20	96.4 (2)
Rh1–S2–C6	116.3 (3)	S1–Rh2–C21	160.1 (2)
Rh2–S2–C6	116.7 (3)	S1–Rh2–C22	99.0 (2)
S1–Rh1–C11	97.7 (2)	S2–Rh2–C19	98.7 (2)
S1–Rh1–C12	156.9 (3)	S2–Rh2–C20	158.3 (2)
S1–Rh1–C13	100.0 (2)	S2–Rh2–C21	97.8 (2)
S1–Rh1–C14	162.7 (3)	S2–Rh2–C22	162.2 (2)

Results and Discussion

Preparation and Molecular Structure of $[Rh_2(\mu\text{-}S(CH_2)_3NMe_2)_2(cod)_2]$. The dinuclear complex $[Rh_2(\mu\text{-}S(CH_2)_3NMe_2)_2(cod)_2]$ (1) has been prepared by reaction of

(9) Garst, M. E.; Lukton, D. *J. Org. Chem.* **1981**, *46*, 4433.
(10) Van Leeuwen, P. W. N. M.; Roobeck, C. F. *J. Organomet. Chem.* **1983**, *258*, 343.
(11) Kalck, Ph.; Frances, J. M.; Pfister, P. M.; Southern, T. G.; Thorez, A. *J. Chem. Soc., Chem. Commun.* **1983**, 510.
(12) (a) Kalck, Ph. In *Organometallics in Organic Synthesis*; de Meijere, A., tom Dieck, H., eds.; Springer-Verlag: Berlin, 1988; pp 297–320. (b) Kalck, Ph.; Thorez, A.; Pinillos, M. T.; Oro, L. A. *J. Mol. Catal.* **1987**, *43*, 1.
(13) Bayón, J. C.; Real, J.; Claver, C.; Polo, A.; Ruiz, A. *J. Chem. Soc., Chem. Commun.* **1989**, 1056.
(14) (a) Lazzaroni, R.; Bertozzi, S.; Pocai, P.; Troiani, F.; Salvadori, P. *J. Organomet. Chem.* **1985**, *295*, 371. (b) Amer, I.; Alper, H. *J. Am. Chem. Soc.* **1990**, *112*, 3674.
(15) (a) Vietti, D.; Ill, C. U.S. Patent 4376208, 1983. (b) Volf, E. Y.; Soloveva, T. Y.; Vartanyan, M. M.; Brezhnev, L. Y.; Lapidus, A. L. *Izv. Akad. Nauk SSSR, Ser. Khim.* **1989**, *11*, 2569.
(16) (a) Falbe, J.; Korte, F. *Chem. Ber.* **1964**, *97*, 1104. (b) Stapp, P. R.; Allen, J. D. U.S. Patent 3555048, 1971, *Chem. Abstr.* **1971**, *75*, 5702.
(17) Amino, Y.; Nishi, S.; Izawa, K. *Bull. Chem. Soc. Jpn.* **1991**, *64*, 620.

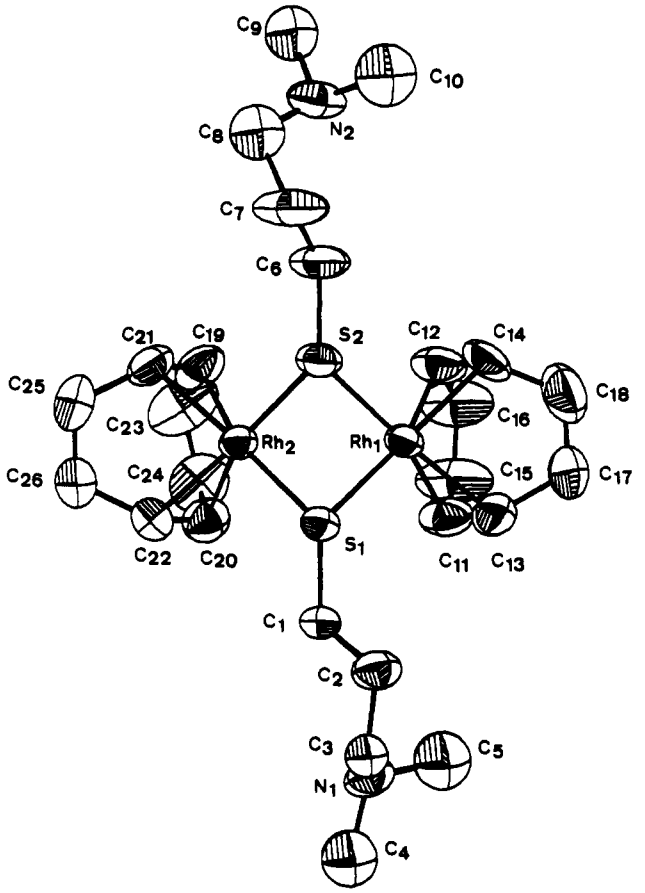

Figure 1. Molecular structure of the precursor catalyst complex $[Rh_2(\mu\text{-}S(CH_2)_3NMe_2)_2(cod)_2]$ (1).

a solution of $[Rh_2(\mu\text{-}Cl)_2(cod)_2]$ in dichloromethane with a stoichiometric amount of dimethyl(3-mercaptopropyl)-amine, $HS(CH_2)_3NMe_2$, and potassium *tert*-butoxide in methanol. The compound was isolated as a yellow-orange air-stable crystalline solid.

The crystal structure consists of discrete dinuclear units separated by van der Waals contacts. The coordination about each rhodium atom is approximately square-planar. Two bridging sulfur atoms and a chelating cyclooctadiene are ligated to each metal atom, and none of the amine groups are involved in the coordination. The Rh_2S_2 ring is highly puckered, the dihedral angle between the planes S1Rh1Rh2 and S2Rh1Rh2 being 104.7 (1)°. The amine-thiolato bridging groups are in a syn configuration with respect to the four-membered Rh_2S_2 core.

A view of the molecule with the atom-labeling scheme is shown in Figure 1. Table I shows the atom positions for the structure of $[Rh_2(\mu\text{-}S(CH_2)_3NMe_2)_2(cod)_2]$, and Table II lists the most significant intramolecular distances and bond angles with their standard deviations.

The Rh–S bond lengths average 2.34 Å. These are slightly shorter than those found in closely related dinuclear thiolato-bridged complexes. The longest related bond was reported for $[Rh_2(\mu\text{-}SC_6F_5)_2(cod)_2]$ (average 2.41 Å).[18] More comparable Rh–S bond distances were observed in the mixed carbonyl phosphine complex *cis*-$[Rh_2(\mu\text{-}SPh)_2(CO)_2(PMe_3)_2]$ (average 2.387 Å)[19] and especially in the tetracarbonyl derivative $[Rh_2(\mu\text{-}SC_6H_4F)_2(CO)_4]$ (average 2.36 Å).[20] The Rh–C distances (2.12–2.14 Å) are in the range reported for other Rh(I) complexes containing cod ligands trans to S donor atoms.[18,21] The intramolecular Rh–Rh distance (2.96 Å) suggests the existence of some metal–metal interactions and is very similar to the intermetallic distances found in $[Rh_2(\mu\text{-}SC_6F_5)_2(cod)_2]$ (average 2.955 Å)[18] and $[Rh_2(\mu\text{-}SC_6H_4F)_2(CO)_4]$ (average 2.960 Å).[20]

Table III. Hydroformylation of 2,3-Dihydrofuran (2) Using 1 + nPR_3[a]

n	PPh_3	$P(OPh)_3$	$P(OMe)_3$	$P(OPh^*)_3$[b]	TPP[c]
2	59 (58/42)	99 (49/51)	76 (57/43)	54 (80/20)	64 (72/28)
4	88 (56/44)	99 (52/48)	67 (46/54)	98 (75/25)	59 (71/29)
10	58 (49/51)	62 (61/39)	13 (29/71)	99 (76/24)	56 (70/30)
20				100 (77/23)	

[a] Conversions are given in units of mole percent. 4/5 ratios are given in parentheses and were determined by GLC. Reactions were run with 20 mmol of substrate and 0.05 mmol of catalyst precursor 1 in 15 mL of 1,2-dichloroethane at 5 bar and 80 °C for 20 h; molar ratio $CO/H_2 = 1$. [b] Tris(*o-tert*-butylphenyl) phosphite. [c] 1,2,5-Triphenylphosphole.

Table IV. Hydroformylation of 2,5-Dihydrofuran (3) Using 1 + nPR_3[a]

n	PPh_3	$P(OPh)_3$	$P(OMe)_3$	$P(OPh^*)_3$[b]	TPP[c]
2	59 (58/42)	70 (55/45)	58 (17/83)	98 (69/31)	62 (66/34)
4	48 (15/85)	88 (45/55)	59 (10/90)	98 (64/36)	42 (67/33)
10	51 (21/79)	64 (32/68)	43 (1/99)	97 (65/35)	48 (66/34)
20	30 (6/94)				

[a] Conversions are given in units of mole percent. 4/5 ratios are given in parentheses and were determined by GLC. Reactions were run with 20 mmol of substrate and 0.05 mmol of catalyst precursor 1 in 15 mL of 1,2-dichloroethane at 5 bar and 80 °C for 20 h; molar ratio $CO/H_2 = 1$. [b] Tris(*o-tert*-butylphenyl) phosphite. [c] 1,2,5-Triphenylphosphole.

Scheme I

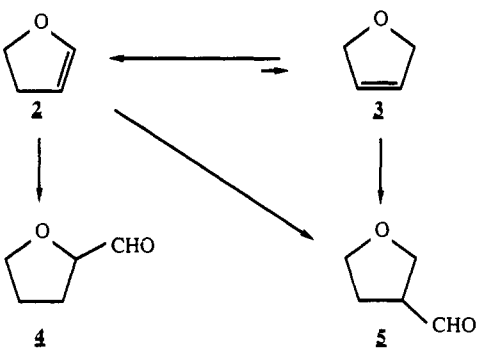

Hydroformylation of Dihydrofurans.[22] Preliminary experiments were undertaken to establish the influence of both the nature of the phosphorus cocatalyst and the Rh:P molar ratio on the hydroformylation of 2,3-dihydrofuran (**2**) and 2,5-dihydrofuran (**3**). For these experiments, low pressures (5 bar) and moderate temperatures (80 °C) were used. The results are shown in Tables III and IV. None of the experiments produced hydrogenation products, and therefore only tetrahydrofuran-2-carbaldehyde (**4**) and tetrahydrofuran-3-carbaldehyde (**5**) were produced.

(18) Cruz-Garritz, C.; Rodríguez, B.; Torrens, H.; Leal, J. *Transition Met. Chem.* **1984**, *9*, 284.

(19) Bonnet, J. J.; Kalck, Ph.; Poilblanc, R. *Inorg. Chem.* **1977**, *16*, 1514.

(20) Claver, C.; Masdeu, A.; Ruiz, N.; Foces-Foces, C.; Cano, F. H.; Apreda, M. C.; Oro, L. A.; García-Alejandre, J.; Torrens, H. *J. Organomet. Chem.* **1990**, *398*, 177.

(21) (a) Claver, C.; Ruiz, A.; Masdeu, A.; Viñas, J.; Saballs, T.; Lahoz, F.; Plou, F. J. *J. Organomet. Chem.* **1989**, *373*, 269. (b) Pinillos, M. T.; Jarauta, M. P.; Oro, L. A.; Tiripicchio, A.; Tiripicchio-Camellini, M. *J. Organomet. Chem.* **1988**, *339*, 181.

(22) A preliminary report has been published: Polo, A.; Real, J.; Claver, C.; Castillón, S.; Bayón, J. C. *J. Chem. Soc., Chem. Commun.* **1990**, 631.

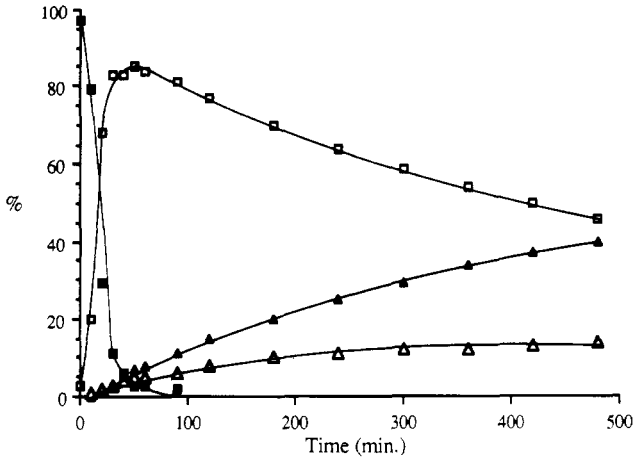

Figure 2. Evolution of the hydroformylation reaction in mole percent of 2,5-dihydrofuran (**3**): (■) 2,5-dihydrofuran; (□) 2,3-dihydrofuran; (▲) tetrahydrofuran-2-carbaldehyde; (△) tetrahydrofuran-3-carbaldehyde. Reaction conditions: 200 mmol of **3**, 0.05 mmol of catalyst, 2 mmol of $P(OPh^*)_3$ in 15 mL of 1,2-dichloroethane; pressure 5 bar; molar ratio CO/H_2 = 1; temperature 80 °C.

In the hydroformylation of 2,3-dihydrofuran, the best conversions were achieved when aryl phosphites were used as cocatalysts. With regard to the selectivity of the reaction, it is interesting to notice the difference in behavior of the bulkier ligands tris(*o-tert*-butylphenyl) phosphite ($P(OPh^*)_3$) and 1,2,5-triphenylphosphole (TPP) when compared with less sterically demanding ligands. In the case of the former, the selectivity of the reaction is not modified on addition of different excesses of ligand, which indicates that a single catalytic species is responsible for reaction under these conditions. Also, the bulky ligands gave the best selectivities toward **4**. In contrast, for the use of trimethyl phosphite ($P(OMe)_3$), the cocatalyst which has the smallest cone angle, the reaction shows the highest dependence of the selectivity on the excess of the phosphite ligand added, giving increased amounts of **5** with increased P:Rh molar ratio. However, when a large excess of phosphite was used, the conversion was much reduced. In the case of triphenylphosphine (PPh_3) or triphenyl phosphite ($P(OPh)_3$), only a slight variation of the selectivity was observed with excess added ligand. Increasing the molar ratios of the phosphorus ligand to rhodium resulted in higher yields of **5** with PPh_3 and of **4** with $P(OPh)_3$.

In the hydroformylation of 2,5-dihydrofuran the highest conversions were also achieved when aryl phosphites were used as cocatalysts. For this alkene a single hydroformylation product, **5**, was expected. However, in all cases, both **4** and **5** were obtained. This result can be explained by considering that an isomerization process is taking place simultaneously with the hydroformylation reaction, as shown in Scheme I.[23] Furthermore, when either $P(OPh^*)_3$ or TPP was used as cocatalyst, the isomerization was faster than the hydroformylation, since a similar product distribution was obtained from either **2** or **3**. In order to find out more about the isomerization process, the reaction mixture was analyzed at different reaction times (Figure 2). Extensive isomerization of **3** to give **2** was observed at the beginning of the reaction, essentially before hydroformylation had begun. It should be noted that fast isomerization takes place only under

Scheme II

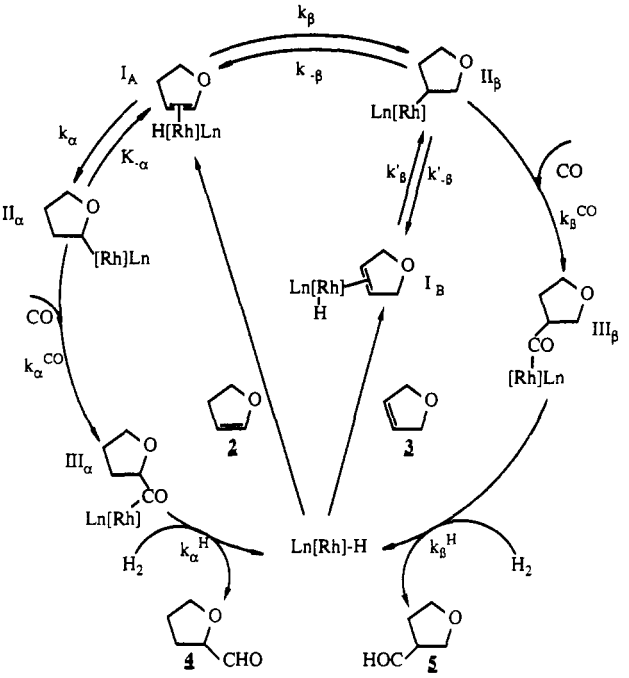

hydroformylation conditions: the presence of the catalyst, hydrogen, and carbon monoxide is required; otherwise, **3** is stable.

As before, for the bulkier cocatalysts, selectivities are independent of the excess of the ligand used. As noted for the hydroformylation of **2**, good selectivities for the aldehyde **5** were achieved when large excesses of PPh_3 or $P(OMe)_3$ were used.

The hydroformylation of vinyl ethers has been studied, but a satisfactory explanation of the observed regioselectivity has not yet been provided.[14a] However, different models have been proposed to explain the regioselectivity in the hydroformylation of polarized alkenes. A simple model suggests a relationship between the regioselectivity observed and the orientation of the dipoles of the polarized alkene and the metal–hydride bond.[7] Pittman[24] proposed that selectivity in the hydroformylation of methyl methacrylate using a rhodium–phosphine catalyst could be explained by considering the equilibrium between the two active species, $[RhH(CO)(PPh_3)_2]$ and $[RhH(CO)_2(PPh_3)]$, which may be modified by changing the concentration of PPh_3:

$$RhH(CO)(PPh_3)_2 \underset{-CO}{\overset{+CO}{\rightleftharpoons}} RhH(CO)_2(PPh_3)_2 \underset{+PPh_3}{\overset{-PPh_3}{\rightleftharpoons}} RhH(CO)_2(PPh_3)$$

These two complexes have metal–hydride bonds with different polarities and thus react to give the metal–*n*-alkyl and –branched-alkyl intermediates with different selectivities.

More recently, Ojima[25] proposed that the regioselectivity of the hydroformylation of fluoroalkenes can be rationalized by considering the stability of the branched-alkyl–metal complex, its tendency to isomerize (i.e. the rate of β-elimination), and the ratio between the rates of formation of the two metal–acyl intermediates. Interestingly, the β-elimination rates for the *n*-alkyl– and branched-alkyl–metal complexes formed during the hydroformylation of

(23) Different metal complexes catalyze the isomerization of allyl to vinyl ethers. See for instance: Davies, S. G. *Organotransition Metal Chemistry Applications to Organic Synthesis*; Pergamon Press: Oxford, U.K., 1982; pp 285–287.

(24) Pittman, Ch. U., Jr.; Honnick, W. D.; Young, J. J. *J. Org. Chem.* **1980**, *45*, 684.

(25) Ojima, I.; Kato, K.; Okabe, M.; Fuchikami, T. *J. Am. Chem. Soc.* **1987**, *109*, 7714 and references cited therein.

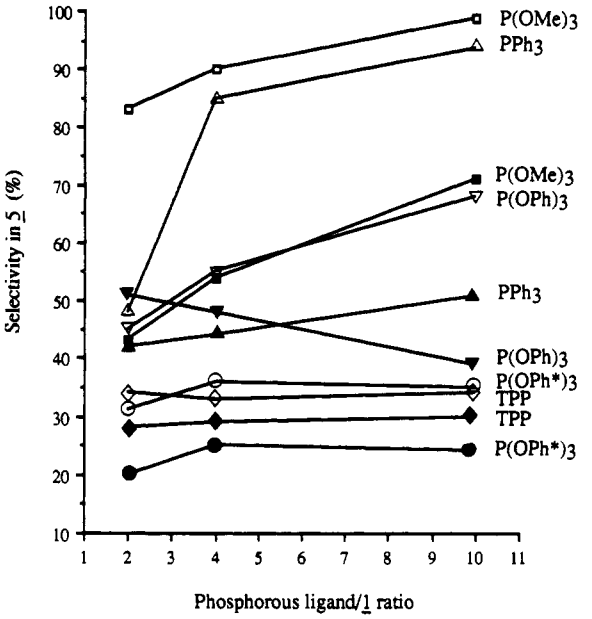

Figure 3. Dependence of the selectivity in the hydroformylation of 2,3-dihydrofuran (2) (solid symbols) and 2,5-dihydrofuran (3) (open symbols) on the nature and relative amount of the phosphorus ligand.

styrene have been shown to be significantly different.[26] We show an integrated model, depicted in Scheme II, based on the regioselectivity observed and inspired by Ojima's model, which allows us to rationalize the results obtained in the hydroformylation of 2,3- and 2,5-dihydrofuran.

The vinyl ether substrate **2** is an almost flat, strongly polarized, and electron-rich conjugated alkene. Because of its cyclic structure, it can be considered that the two possible sites for hydroformylation cannot be discriminated on steric grounds. When the alkene **2** reacts with the metal–hydride complex, the η^2-alkene complex I_A is formed (Scheme II). It can evolve to give either of the metal–alkyl intermediates II_α and II_β. The derivative II_β is thermodynamically favored because the new metal–carbon bond is formed at the carbon with the higher electron density,[25] regardless of the phosphorus ligand used. However, because the C2–metal bond in II_α is more polarized than the C3–metal bond in II_β, the formation of the acyl complex III_α from II_α is faster than the same process for the β species ($K_\alpha^{CO} > K_\beta^{CO}$). On the other hand, the alkyl complex II_β is the only one formed from the metal–alkene intermediate I_B formed in the first step in the hydroformylation of 2,5-dihydrofuran (**3**). Therefore, the hydroformylation of **2** and **3** can be considered as a part of the same catalytic cycle (Scheme II). Given this model, as a first approximation the final product distribution should reflect the ratio of the metal–acyl species III_α and III_β, provided that the hydrogen pressure is high enough so that the hydrogenolysis of the metal–acyl complex is not the rate-determining step.

In the case of the reaction in the presence of $P(OPh^*)_3$, the results shown in Tables III and IV suggest that II_α and II_β are in preequilibrium. This would imply that both β-elimination processes are faster than the acyl formation. In this situation, the aldehyde **4** is preferentially obtained because the acyl complex III_α is formed more rapidly than is III_β. When increasing amounts of $P(OMe)_3$ are used as the addend, aldehyde **5**, which arises from the more stable alkyl complex II_β, becomes the main reaction product, indicating that the β-elimination is slower than the formation of the acyl complex. Significantly, when the $P(OMe)_3$/**1** molar ratio is 10, the hydroformylation of 2,5-dihydrofuran (**3**) gives exclusively the aldehyde **5**; thus, there is no β-elimination. With PPh_3 and $P(OPh)_3$ there is an intermediate situation. The dependence of the regioselectivity on the phosphorus cocatalyst (Figure 3) can be better explained by considering mainly their steric requirements rather than their electronic effects.[27] The remarkably different results obtained with the electronically related aryl phosphine ligands $P(OPh)_3$ and $P(OPh^*)_3$ and the preferred formation of the aldehyde **5** when using the more basic PPh_3 in the hydroformylation of 2,3-dihydrofuran prove that electronic effects are not enough to justify the regioselectivity of these reactions.

Table V. Effect of Total Pressure, CO:H_2 Molar Ratio, and Temperature on the Selectivity of the Hydroformylation of 2,3-Dihydrofuran (2) Using 1 + 4$P(OPh^*)_3$[a]

total pressure, bar	temp, °C	CO/H_2	time, h	[4]/[5],[b] mol %
5	40	1	20	60/40
5	80	1	20	75/25
30	40	1	8	55/45
30	80	1	8	57/43
30	120	1	8	62/38
5	80	2	20	79/21[c]
5	80	1	20	75/25
5	80	0.5	20	72/28

[a] Reactions were run with 20 mmol of substrate and 0.05 mmol of catalyst precursor **1** in 15 mL of 1,2-dichloroethane. $P(OPh^*)_3$ = tris(*o-tert*-butylphenyl) phosphite. Conversion was 97–100%, except where noted. [b] Determined by GLC. [c] Conversion 42%.

A possible explanation can be proposed by considering that, in the case of $P(OPh^*)_3$, the *pair of unique* metal–alkyl intermediates would be coordinatively unsaturated because the size of this ligand prevents the coordination of an extra bulkyl phosphite. Since hydrido(η^2-alkene)-metal complexes are more sterically demanding than the η^1-alkyl species, when using $P(OPh^*)_3$ the β-elimination processes will be favored in comparison with the case for less hindered phosphorus ligands. For the latter, two or more active species coexist with their corresponding alkyl intermediates. An excess of the ligand will shift the equilibrium toward the most coordinatively saturated species. Thus, the β-elimination processes will be disfavored (i.e. acyl formation becomes competitive) and increasing selectivities in the 3-formyl derivative will be obtained on starting from 2,5-dihydrofuran.[28]

The excellent conversions yielded by the use of $P(OPh^*)_3$ as cocatalyst, together with the fact that when this ligand is used a single active species is formed, prompted us to focus on this catalytic system. In other systems, where it has been proposed that more than one catalytic species coexist, a variation in the conditions (for example in pressure and/or temperature) will produce both a

(26) Lazzaroni, R.; Settembolo, R.; Raffaelli, A.; Pucci, S.; Vitulli, G. *J. Organomet. Chem.* **1988**, *329*, 357.

(27) Tolman, C. A. *Chem. Rev.* **1977**, *77*, 313.

(28) Although the true nature of the intermediates is unknown, it can be speculated that in the case of the bulky phosphine the 2-tetrahydrofuryl and 3-tetrahydrofuryl square-planar metal–alkyl intermediates do not have enough room for an extra phosphite ligand, through neither pentacoordination nor substitution of a CO ligand. However, the vacant coordination site is big enough to allow the formation of pentacoordinated η^2-alkene hydride species, which would be in fast equilibria with their respective alkyl intermediates. Conversely, in the case of the less sterically demanding phosphorus cocatalyst, for each alkyl intermediate, at least two species with different numbers of phosphorus ligands would coexist. When the P:Rh molar ratio is increased, the more hindered species would become dominant, and for those the β-elimination is disfavored when compared with the formation of the acyl complex.

Table VI. Effect of the Total Pressure and Substrate/Catalyst Molar Ratio on the Selectivity[a] of Hydroformylation[b] of 2,5-Dihydrofuran (3) with the System 1 + 10PPh$_3$

subst/cat	pressure, bar	temp, °C	time, h	conversn, %	[4]/[5], mol %
400	5	80	20	51	21/79
100	5	80	20	67	11/89
400	30	80	8	94	10/90
100	30	80	8	99	1/99

[a] Determined by GLC. [b] Reactions were run with 20 mmol of substrate and 0.05 mmol of catalyst precursor 1 in 15 mL of 1,2-dichloroethane.

Table VII. Effect of the Temperature and the Phosphorus Ligand/Catalyst Ratio on the Selectivity[a] of the Hydroformylation[b] of 2,3-Dihydrofuran (4) and 2,5-Dihydrofuran (5) Using 1 + nP(OPh*)$_3$[c,d]

substrate	n	4/5, mol % 30 °C	40 °C	60 °C	80 °C
4	4		60/40	70/30	75/25
	10		63/37	71/29	76/24
	20		64/36	71/29	77/23
5	4	20/80			72/28

[a] Determined by GLC. [b] Reactions were run with 20 mmol of substrate and 0.05 mmol of catalyst precursor 1 in 15 mL of 1,2-dichloroethane at 5 bar for 20 h, for a molar ratio CO/H_2 = 1. [c] Tris(*o-tert*-butylphenyl) phosphite. [d] Yield 98–100% in all cases.

change in the inherent selectivity from each one of the catalytic species and a shift in the equilibrium between them. Since these effects may be in the same or opposite direction, optimization of the reaction becomes complex and requires very extensive variation of all the parameters.

Effects of Pressure and Temperature. At a constant temperature an increase of the total pressure raises the rate of acyl formation because of the higher partial pressure of CO. In this situation, CO insertion is much faster than β-elimination, and the product distribution of the hydroformylation of the alkene 2 approaches a dependence on the relative rates of formation of II_α and II_β (Table V). For 3 the formation of aldehyde 5 becomes dominant (Table VI). Therefore, for both alkenes the selectivity for 5 increases. Moderate changes in CO/H_2 partial pressures show little effect on the selectivity of the reaction (Table V).

When the temperature was increased, higher selectivity for the formation of 4 was observed. Thus, in the range of temperatures explored (Tables VI and VII) it seems that only the β-elimination is significantly affected. Therefore, a fast preequilibrium is established between the metal alkyl species, via the β-elimination process, so that the selectivity is dominated by the faster rate of formation of the acyl III_α, and the selectivity for aldehyde 4 increases.

It is noteworthy that in the case of the P(OPh*)$_3$ cocatalyst the regioselectivity was independent of the excess of the ligand, whatever the reaction temperature was. Less

Scheme III

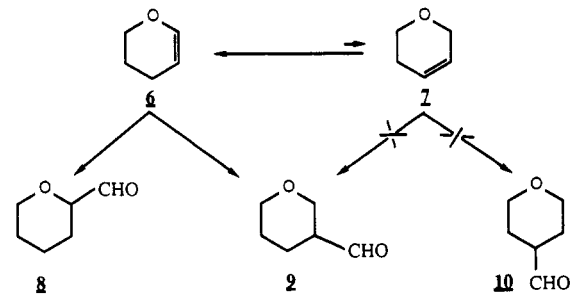

could be deduced from other auxiliary ligands, since they showed negligible activities at low temperatures.

Finally, considering all the reaction parameters, conditions were chosen to optimize yields and selectivities for the aldehydes 4 and 5. Thus, tetrahydrofuran-2-carbaldehyde (4) can be prepared in 77% yield from 2,3-dihydrofuran (2) or from 2,5-dihydrofuran (3) in 72% yield, by using a bulky phosphite, P(OPh*)$_3$, low pressure (5 bar), and moderate temperature (80 °C). On the other hand, tetrahydrofuran-3-carbaldehyde (5) was obtained in quantitative yield from 2,5-dihydrofuran (3) when PPh$_3$ was added, at high pressure (30 bar) and moderate temperature (80 °C). In this case, the alkene/catalyst molar ratio was reduced to 100. In addition to the expected improvement in the conversion, an unanticipated increment in the selectivity was also obtained.

Hydroformylation of Dihydropyrans. The results obtained for the hydroformylation of 3,4-dihydro-2*H*-pyran (6) and 3,6-dihydro-2*H*-pyran (7) are shown in Table VIII. In addition to the aldehydes tetrahydropyran-2-carbaldehyde (8) and tetrahydropyran-3-carbaldehyde (9), other reaction products (including alcohols) were obtained, but always in less than 5% yield.

The hydroformylation of alkenes 6 and 7 required more severe conditions than the ones used for dihydrofurans. Only when P(OPh*)$_3$ was used as cocatalyst were significant conversions achieved.

As with the previously discussed dihydrofurans, a fast isomerization of the allylic ether 7 was observed under hydroformylation conditions (Scheme III). For that reason, the same product distribution was obtained when we started from either 6 or 7. Moreover, tetrahydropyran-4-carbaldehyde (10) was never detected in the final mixtures. In all the cases the aldehyde 8 was the major product. These results indicate that the hydroformylation of 6 and 7 can be described by a catalytic cycle similar to the one shown in Scheme II for dihydrofurans.

The constraints imposed by the low activity of the catalytic system (high pressure and temperature), and the fact that the only useful cocatalyst was P(OPh*)$_3$, permit little control of the regioselectivity of the reaction. For example, the temperature must be maintained at about 120 °C; higher temperatures seem to decompose the catalyst, while at lower temperatures the system is nearly

Table VIII. Hydroformylation of 3,4-Dihydro-2*H*-pyran (6) and 5,6-Dihydro-2*H*-pyran (7)

substrate	catalyst	pressure, bar	temp, °C	CO/H_2	time, h	conversn, %	[8]/[9], mol %
6	1 + 10PPh$_3$	75	120	0.5	8	3	62/38
6	1 + 10P(OPh*)$_3$[a]	35	120	1	8	72	67/33
6	1 + 10P(OPh*)$_3$	75	120	1	8	83	67/33
6	1 + 10P(OPh*)$_3$	35	80	0.5	8	10	75/25
6	1 + 10P(OPh*)$_3$	35	120	0.5	8	76	64/36
6	1 + 10P(OPh*)$_3$	35	160	0.5	8	54	49/51
6	1 + 10P(OPh*)$_3$	35	120	1	8	72	67/33
7	1 + 10PPh$_3$	75	120	0.5	8	3	61/39
7	1 + 10P(OPh*)$_3$	75	120	0.5	8	81	68/32

[a] Tris(*o-tert*-butylphenyl) phosphite.

inactive. Only a few experiments yielded appreciable conversions, with a rather narrow range of selectivities. Thus, any attempt to rationalize the influence of the reactions is very difficult.

The remarkable difference in reactivity between the dihydrofurans and the dihydropyrans can be attributed to the planarity of the former, when compared with the nonplanar six-membered-ring dihydropyrans. In order to gain some insight on this point, the hydroformylation of 3,4-dihydro-4,4-dimethyl-2*H*-pyran-2-one (11) was undertaken.

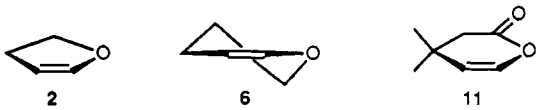

2 6 11

Because of the presence of three sp^2 carbons, the alkene 11 is a more rigid and planar ring, favoring coordination to the metal center. For that reason, even at 5 bar and 80 °C, a 55% conversion to aldehydes was achieved (92% of the 6-formyl derivative 12). Under these mild conditions, dihydropyrans 6 and 7 do not react. The reactivity of substrate 11 is remarkable when one considers that it is a more hindered and less electron-rich alkene than the dihydropyrans 6 and 7. Therefore, the coordination of the alkene seems to be a critical step in the rate of hydroformylation of dihydropyrans.

The Problem of the Catalytic Species. A catalytic cycle for the hydroformylation of alkenes with binuclear rhodium thiolato complexes has been proposed on the basis of theoretical calculations and some experimental evidence.[12a,29] In this model the complexes $[Rh_2(\mu\text{-}SR)_2(CO)_2(PR_3)_2]$ are the active catalysts and the dinuclear unit is maintained in all the intermediates in the catalytic cycle. The first step involves the oxidative addition of H_2 to one of the Rh atoms, while the other metal center binds the alkene. The first hydride is directly transferred to the coordinated alkene to form the alkyl complex, which undergoes one-center migration to the CO ligand, giving the acyl species. The second hydride transfer takes place through an intermediate containing a single thiolato and a hydride bridge, produced by cleavage of one of the bonds of the thiolato bridging ligands. Finally, the double-thiolato-bridged system is regenerated, the aldehyde is eliminated from the Rh(III) center, and the Rh(I) center undergoes a new oxidative addition of H_2.

In spite of the differences of this cycle from that proposed for Wilkinson's catalyst, both cycles involve essentially the same basic steps: coordination of the alkene and formation of an alkyl complex, formation of the acyl complex, and reductive elimination of the aldehyde. A preliminary step is required in the dinuclear complex to form a hydride, but since this step does not discriminate between the paths leading to either of the isomeric aldehydes (Scheme II), *the arguments used to justify the regioselectivity of the reaction should be valid, whether the mechanism goes through mononuclear species (i.e., Wilkinson's type) or through dinuclear species (i.e., dinuclear thiolato bridged).*

We have explored the reactivity of $[Rh_2(\mu\text{-}S(CH_2)_3NMe_2)_2(cod)_2]$ (1) in order to elucidate the nature of the active catalytic species. Complex 1 does not react with an excess of PPh_3, as evidenced by ^{31}P and ^1H NMR spectroscopy. However, 1 reacts with CO at ambient pressure to give the dinuclear complex $[Rh_2(\mu\text{-}S(CH_2)_3NMe_2)_2(CO)_4]$ (13), which has been spectroscopically characterized. The infrared spectrum in the carbonyl region shows the characteristic pattern for a dinuclear folded tetracarbonyl. This complex is not a hydroformylation catalyst in the absence of phosphorus ligands. The reaction of 1 with CO and phosphines or phosphites produces the dinuclear mixed carbonyl phosphine or phosphite compounds $[Rh_2(\mu\text{-}SR)_2(CO)_2(PR_3)_2]$. The same compounds are formed by reaction of the tetracarbonyl complex and the phosphorus ligand. In both cases the reaction is somewhat slow at room temperature, because of the formation of pentacoordinated species $[Rh_2(\mu\text{-}SR)_2(CO)_4(PR_3)_2]$, as previously reported,[30] but the reaction is fast at 80 °C. Significantly, when the bulky phosphite $P(OPh^*)_3$ was used as phosphorus ligand, the reaction was fast even at room temperature, suggesting an intrinsic instability of the pentacoordinated species when this bulky phosphite is one of the ligands. This fact could be related to the fast β-elimination observed when $P(OPh^*)_3$ was used as cocatalyst. The mixed carbonyl phosphorus complexes are very soluble in most common solvents and difficult to crystallize. Thus, they have only been generated in solution and investigated by infrared and NMR spectroscopy. Only when tris(*o*-tolyl)phosphine was the added ligand could the complex be isolated as a pure crystalline material. The ^{31}P NMR spectrum in dichloroethane shows two broad doublets, which can be assigned to the cis and trans isomers in dynamic equilibrium. In the case of the less hindered triphenylphosphine, two sharp doublets at δ 38.9 (J_{Rh-P} = 157 Hz) and 37.1 ppm (J_{Rh-P} = 154 Hz) with relative intensities 3:1 are observed. As expected for a cis/trans equilibrium, the intensity of the signals is not modified upon addition of excess phosphine. In the ^{13}C NMR spectrum, two sets of double doublets of different intensity are observed in the carbonyl region. The more intense is at δ 190.6 ppm (J_{Rh-C} = 74 Hz; J_{P-C} = 16 Hz), while the weaker set of signals is centered at δ 190.2 ppm (J_{Rh-C} = 76 Hz, J_{P-C} = 17 Hz). Each set is characteristic of a CO ligand coordinated to a square-planar rhodium bearing only one phosphorus ligand. The infrared spectrum shows a band at 1965 cm^{-1}, with a shoulder at 1991 cm^{-1}. Interestingly, in the reaction with $P(OPh^*)_3$, a single sharp doublet at δ 118.3 ppm (J_{Rh-P} = 254 Hz) was observed in the ^{31}P NMR spectrum. There is also only a single absorption in the carbonyl region of the infrared spectrum at 1995 cm^{-1}. In the ^{13}C NMR spectrum, the signal for the carbonyl appears as one double doublet at δ 187.1 ppm (J_{Rh-C} = 72 Hz; J_{P-C} = 19 Hz). At this stage, the behavior of the bulky phosphite is analogous to that of the less hindered ligands $P(OMe)_3$ and $P(OPh)_3$. The former shows one doublet at δ 121.5 ppm (J_{Rh-P} = 262 Hz), and the latter at δ 135.1 ppm (J_{Rh-P} = 179 Hz).

In an attempt to follow the evolution of the rhodium species in the hydroformylation process, samples of the catalytic solutions were taken from the reactor and investigated by infrared spectroscopy at ambient pressure. When PPh_3 was used as the addend, the single band corresponding to the dinuclear mixed carbonyl phosphine complex was observed throughout the reaction. Only at the end (over 80% conversion) of the reaction was the band shifted to 1975 cm^{-1}, probably due to a modification of the cis/trans equilibrium. In the case of $P(OPh^*)_3$, the system shows a more complex behavior. The intensity of the initial band at 1995 cm^{-1}, corresponding to the dinuclear carbonyl phosphite species, decreases, while new signals at 2072, 2043, and 2011 cm^{-1} start to appear. Furthermore, in the final solution the relative intensities of these bands

(29) Dedieu, A.; Escaffre, P.; Frances, J. M.; Kalck, Ph.; Thorez, A. *Nouv. J. Chim.* **1986**, *10*, 631.

(30) Kalck, Ph.; Poilblanc, R. *Inorg. Chem.* **1975**, *14*, 2779.

depend on the excess of phosphite used. The band at 2011 cm^{-1} is assigned to *trans*-[RhCl(CO)[P(OPh*)$_3$]$_2$] (**15**) by comparison with an independently prepared sample. Obviously, the chloro ligand is derived from the solvent, and the chlorination is very fast in the presence of P(OPh*)$_3$. In the case of PPh_3 this reaction is observed only after prolonged periods of time. When used as a catalyst, *trans*-[RhCl(CO)[P(OPh*)$_3$]$_2$] exhibits the same conversions and selectivities as **1** + P(OPh*)$_3$. The same results were also obtained when a mixture of [Rh$_2$(μ-OMe)$_2$(cod)$_2$] and P(OPh*)$_3$ was used, and in this case the complex *trans*-[RhCl(CO)[P(OPh*)$_3$]$_2$] was also detected in the final solution. The different nature of the catalytic solutions of **1** + PPh_3 on one hand and **1** + P(OPh*)$_3$ on the other is also confirmed by the fact that, in the hydroformylation of 1-hexene, the first system performs well, giving very high conversions, while the second works very poorly (26% conversion). The complex *trans*-[RhCl(CO)[P(OPh*)$_3$]$_2$] is inactive under these conditions. It does, however, become active (58% conversion) in the presence of Et_3N, which may have the effect of removing the chloride.[31] In this case, bands at 2011 and 2043 cm^{-1} are detected in the IR spectrum of the catalytic solutions. We suggest the band at 2043 cm^{-1} may correspond to a rhodium carbonyl hydride species. Attempts to synthesize and isolate the corresponding [RhH(CO)[P(OPh*)$_3$]$_2$] complex by standard methods have so far failed.

Conclusions

The dinuclear rhodium complex **1** has been used to be an effective catalyst precursor for the hydroformylation of vinyl and allyl cyclic ethers. Depending on the phosphorus cocatalyst used, the catalyst preserves its dinuclear structure or is converted into a mononuclear species.

The planar five-membered ring in dihydrofuran can be hydroformylated at lower pressure and temperature than can the nonplanar, six-membered ring of dihydropyran. Because of the wide range of the reaction conditions which permit the hydroformylation of dihydrofurans, we have been able to show a remarkable dependence of reaction selectivity on the phosphorus cocatalyst, the pressure, and the temperature. A systematic study of these parameters allows us to explain the selectivity of the reaction on the basis of the alkene polarization and the size of the phosphorus ligand used. These two factors determine the stability and the rate of formation of the alkyl complex, and the rates of β-elimination and acyl formation. Finally, the hydroformylation of 2,5-dihydrofuran to tetrahydrofuran-2-carbaldehyde opens a new synthetic route for the introduction of a formyl group in the α-position of allylic substrates.

Experimental Section

All syntheses of rhodium complexes were performed using standard Schlenk techniques under a nitrogen atmosphere. [Rh$_2$(μ-Cl)$_2$(cod)$_2$] and dimethyl(3-mercaptopropyl)amine were prepared by previously described methods. Solvents were purified by standard procedures. All other reagents were commercial samples and were used as purchased. Infrared spectra (KBr pellets or solution) were obtained using a Nicolet 5ZDX spectrophotometer. Elemental analyses were performed on a Perkin-Elmer 240-C analyzer. ^1H and ^{13}C NMR spectra were recorded on a Bruker AM-400 spectrophotometer, and chemical shifts are quoted in ppm downfield from internal TMS. ^{31}P NMR spectra were obtained on the same instrument at 160 MHz, using external 85% H_3PO_4 as reference. Mass spectrometry was performed on a Hewlett-Packard CG/MS 5988A spectrometer, using an Ultra-2 (diphenylsilicone 5%, dimethylsilicone 95%) column. Gas chromatography was performed on a Hewlett-Packard 5840A chromatograph with an OV-17 on Chromosorb WHP 6 m × $^1/_8$ in. column for products **4** and **5** and with a CW 1540 on Chromosorb WNAW 4 m × $^1/_{12}$ in. column for products **8** and **9**.

Preparation of [Rh$_2$(μ-S(CH$_2$)$_3$NMe$_2$)$_2$(cod)$_2$] (1). A solution of potassium *tert*-butoxide (227 mg, 2.03 mmol) and dimethyl(3-mercaptopropyl)amine (0.27 cm^3, 2.03 mmol) in methanol (5 cm^3) was stirred at room temperature for 5 min. This solution was added to a stirred solution of [Rh$_2$(μ-Cl)$_2$(cod)$_2$] (500 mg, 1.01 mmol) in dichloromethane (5 cm^3) at room temperature over 30 min. The reaction mixture was then evaporated, and the resulting oil was extracted with dichloromethane (10 cm^3) and filtered through Celite to eliminate the potassium chloride formed. The orange solution obtained was concentrated to 0.5 cm^3, and acetonitrile was added until a slight cloudiness appeared. The mother liquor was left overnight in a refrigerator, and the orange crystals which had formed were separated by filtration. A second crop of crystals could be obtained from the mother liquor; yield 603 mg of **1** (90%). Anal. Found: C, 47.0; H, 7.4; N, 4.25. Calcd for $C_{26}H_{48}N_2S_2Rh_2$: C, 47.4; H, 7.35; N, 4.25. NMR ($CDCl_3$): ^1H δ 4.15 (m, cod), 2.38 (m, cod), 2.26 (t, NCH_2), 2.13 (s, NMe_2), 2.04 (t, SCH_2), 1.97 (m, cod), 1.64 (q, CH_2); ^{13}C δ 79.1 (cod), 58.9 (NCH_2), 45.4 (NMe_2), 31.5 (cod), 30.5 (SCH_2), 22.5 (CH_2).

Preparation of [Rh$_2$(μ-S(CH$_2$)$_3$NMe$_2$)$_2$(CO)$_4$] (13). A stream of CO was bubbled through a solution of **1** (50 mg, 0.076 mmol) in methanol (3 mL), and a rapid change of color to red-orange was observed. When this solution was left overnight at −24 °C, crystals were formed, and these were collected by filtration at −50 °C to give 32 mg (84% yield) of a red product which became violet-black on warming. IR ν(CO): in KBr, 2062, 2042, 2003 cm^{-1}; in CH_2Cl_2 solution, 2074, 2054, 2006 cm^{-1}. NMR (CD_2Cl_2): ^1H δ 3.12 (t, J = 7 Hz, NCH_2), 2.44 (t, J = 7 Hz, SCH_2), 2.24 (s, NCH_3), 1.98 (quint, J = 7 Hz, CH_2); ^{13}C δ 184.7 (d, J_{Rh-C} = 70 Hz, CO), 58.2 (NCH_2), 45.4 (NMe), 34.0 (SCH_2), 31.8 (CH_2).

Preparation of [Rh$_2$(μ-S(CH$_2$)$_3$NMe$_2$)$_2$(CO)$_2$(P(*o*-MeC$_6$H$_4$)$_3$)$_2$] (14). Carbon monoxide was bubbled through a solution of **1** (40 mg, 0.06 mmol) and tris(*o*-tolyl)phosphine (37 mg, 0.12 mmol) in CH_2Cl_2. The solution was concentrated, and MeOH was added. Cooling to −24 °C caused the formation of a yellow microcrystalline solid that was isolated by filtration, washed with cold MeOH, and vacuum-dired; yield 55 mg (82%). Anal. Found: C, 58.9; H, 6.05; N, 2.44. Calcd for $C_{54}H_{66}N_2O_2P_2S_2Rh_2$: C, 58.6; H, 6.01; N, 2.53. IR ν(CO): in KBr, 1957 cm^{-1}. NMR (CD_2Cl_2): ^1H δ 7.10–7.40 (m, Ph), 2.37 (s, NCH_3), 1.98 (s, CH_3), 1.87 (m, NCH_2), 1.58 (m, CH_2), 1.26 (m, SCH_2); ^{31}P δ 32.0 (J_{Rh-P} = 150 Hz), 30.5 (J_{Rh-P} = 163 Hz).

Preparation of RhCl(CO)(P(OBu^{t}C$_6$H$_4$)$_3$)$_2$ (15). A stream of CO was bubbled through a solution of [Rh$_2$(μ-Cl)$_2$(cod)$_2$] (50 mg, 0.1 mmol) in dichloromethane (5 mL), and then tris(*o*-*tert*-butylphenyl) phosphite (196 mg, 0.4 mmol) was added. A brisk gas evolution and a change of color to pale yellow was observed. After 5 min, ethanol (5 mL) was added and the solution was concentrated until a solid appeared. The solid formed was filtered, washed with cold ethanol, and dried, yielding 226 mg (100% yield) of **15**. Anal. Found: C, 65.6; H, 7.07. Calcd for $C_{61}H_{78}O_7P_2ClRh$: C, 65.2; H, 7.00. IR ν(CO): in KBr, 2008 cm^{-1}; in CH_2Cl_2 solution, 2011 cm^{-1}. NMR ($CDCl_3$): ^1H δ 7.70, 7.30, 6.90 (d, d, m, Ph), 1.40 (s, CH_3); ^{13}C δ 182.5 (m, CO, J_{Rh-CO} = 70 Hz, J_{P-CO} = 20 Hz), 150.5, 139.4, 127.4, 126.6, 124.0, 120.8, 34.9, 30.5; ^{31}P δ 112.0 (d, J_{Rh-P} = 213 Hz).

Catalysis. Low-pressure hydroformylation experiments (5 and 35 bar) were carried out in a specially designed autoclave with magnetic stirring. The catalytic solution was contained in a glass vessel. The inside part of the cover is made from Teflon to protect the solution from direct contact with the stainless steel. Constant temperature was maintained by the circulation of water through a double jacket. The gas mixture was introduced at constant pressure from a gas ballast. The drop of pressure in the ballast was monitored using a pressure transducer connected to an electronic measurement and printing unit.

High-pressure hydroformylation experiments (75 bar) were carried out in a Berghof autoclave, and the reaction mixtures were magnetically stirred and electrically heated. These experiments were not performed at constant pressure, but for the amount of

(31) Bayón, J. C.; Esteban, P.; Real, J.; Claver, C.; Polo, A.; Ruiz, A.; Castillón, S. *J. Organomet. Chem.* **1991**, *403*, 393.

Table IX. Summary of Crystal Data for $[Rh_2(\mu\text{-}S(CH_2)_3NMe_2)_2(cod)_2]$

formula	$C_{26}H_{48}S_2N_2Rh_2$
mol wt	658.62
cryst syst	monoclinic
space group	$C2/C$ (No. 15)
a, Å	22.543 (4)
b, Å	12.040 (2)
c, Å	21.574 (3)
β, deg	98.77 (1)
V, Å^3	5787.1
Z	8
d_{calc}, g cm^{-3}	1.51
μ(Mo Kα), cm^{-1}	12.78
radiation	graphite-monochromated Mo Kα, λ = 0.71069 Å
scan type	$\omega/2\theta$
2θ range, deg	5–50
scan width, deg	0.8 + 0.35 tan θ
scan speed, deg/min	8.24
total no. of data	5498
o. of unique data, $I > 3\sigma(I)$	4091
no. of params	311
R	0.041
R_w	0.044
abs cor, min–max	0.974–0.832

substrate used the drop of pressure was never more than 3 bar.

Standard Experiment. A solution of the substrate (20 mmol), previously stirred with alumina for 24 h, the catalyst (0.05 mmol), and the phosphorus cocatalyst was introduced into the evacuated autoclave and heated with stirring. Once the system reached thermal equilibrium, the gas mixture was introduced to reach the working pressure. Small samples of the catalytic solution were taken at various intervals to be analyzed. After each run, the solution was removed from the autoclave and analyzed by FT-IR spectroscopy, gas chromatography, and ^{1}H and ^{13}C NMR spectroscopy.

Tetrahydrofuran-2-carbaldehyde (**4**) and tetrahydrofuran-3-carbaldehyde (**5**) were identified by GC and comparison to authentic samples prepared by oxidation of the corresponding alcohols, by mass spectrometry, and by preparation and isolation of the 2,4-dinitrophenylhydrazone derivatives.

MS: **4**, m/e 100 (M^+) (35%), 99 ($M^+ - 1$) (30%), 71 ($M^+ - 29$) (100%); **5**, m/e 71 ($M^+ - 29$) (100%).

4 (as the 2,4-dinitrophenylhydrazone): mp 123–124 °C. Anal. Found: C, 47.4; H, 4.30; N, 20.2. Calcd for $C_{11}H_{12}N_4O_5$: C, 47.1; H, 4.29; N, 20.0. NMR ($CDCl_3$): ^{1}H (300 MHz) δ 11.05 (1 H, s, NH), 9.12 (1 H, d, $J_{3',5'}$ = 2.5 Hz, H-3′), 8.32 (1 H, dd, $J_{5',6'}$ = 9.6 Hz, H-5′), 7.94 (1 H, d, H-6′), 7.45 (1 H, d, $J_{CH=N,3}$ = 5.6 Hz, CH=N), 4.61 (1 H, m, H-2), 3.95 (2 H, m, H-5), 1.97–2.27 (4 H, m, H-3, H-4); ^{13}C (75 MHz) δ 150.8, 144.9, 138.4, 129.8, 123.4, 116.5, 77.25, 68.25, 30.1, 25.9.

5 (as the 2,4-dinitrophenylhydrazone): mp 121–122 °C. Anal. Found: C, 47.3; H, 4.33; N, 20.1. Calcd for $C_{11}H_{12}N_4O_5$: C, 47.1; H, 4.29; N, 20.0. NMR ($CDCl_3$): ^{1}H (300 MHz), δ 11.06 (1 H, s, NH), 9.08 (1 H, d, $J_{3',5'}$ = 2.7 Hz, H-3′), 8.24 (1 H, dd, $J_{5',6'}$ = 9.5 Hz, H-5′), 7.90 (1 H, d, H-6′), 7.54 (1 H, d, $J_{CH=N,3}$ = 6 Hz, CH=N), 4.04–3.82 (4 H, m, H-2, H-4), 3.27 (m, H-3), 2.34–2.02 (2 H, m, H-4); ^{13}C (75 MHz) δ 152.0, 142.7, 129.9, 123.4, 116.4, 70.5, 68.0, 42.1, 30.4.

Tetrahydropyran-2-carbaldehyde (**8**), tetrahydropyran-3-carbaldehyde (**9**), and 3,4-dihydro-4,4-dimethyl-6-formyltetrahydropyran-2-one (**12**) were identified by GC–mass spectrometry: **8**, shows no M^+ or $M^+ - 1$ peaks, and m/e 85 ($M^+ - 29$) (100%); **9**, m/e 114 (M^+), 113 ($M^+ - 1$), 96 ($M^+ - 18$), 95 ($M^+ - 19$), 83 (100%); **12**, m/e 156 (M^+) (1%), 127 ($M^+ - 29$) (100%), 99 (35%), 83 (7%).

Crystal Structure Determination of $[Rh_2(\mu\text{-}S(CH_2)_3NMe_2)_2(cod)_2]$. X-ray-quality crystals were grown by slow diffusion of CH_3CN into a CH_2Cl_2 solution. Crystal data, data collection parameters, and the results of the calculations for the structure solution and refinement are given in Table IX. All measurements were done at 23 °C. Unit cell dimensions were determined by least-squares refinement of the positional parameters for 25 reflections. Three standard reflections were collected every 2 h, and no significant decay was observed. All the data were corrected for Lorentz and polarization effects. An empirical correction for the absorption effect was performed at an advanced state of the structural refinement by using the program DIFABS.[32] Atomic scattering factors are those tabulated by Cromer and Waber.[33]

The structure was solved by Patterson methods. After the location of all the non-hydrogen atoms from F_o and ΔF maps, the full-matrix least-squares refinement was performed. Some disorder affects the carbon atoms linked α to the two nitrogen atoms. A double image was detected for these atoms in ΔF maps, and the fractional population parameters were refined to 0.7 and 0.3, respectively. Every second member of each pair of disordered atoms is distinguished by a double prime in Table I. All nondisordered atoms were refined anisotropically. Most of the hydrogen atoms were introduced at calculated positions, but the H atoms linked to the disordered C atoms were ignored. The final ΔF map was featureless.

Acknowledgment. This research was supported by DGICYT (Ministerio de Educación y Ciencia, Spain), Grants PB 86-0137-C02 and PB-88-0252.

Registry No. **1**, 143289-08-1; **2**, 1191-99-7; **3**, 1708-29-8; **4**, 7681-84-7; **4** 2,4-dinitrophenylhydrazone, 91141-80-9; **5**, 79710-86-4; **5** 2,4-dinitrophenylhydrazone, 104295-75-2; **6**, 110-87-2; **7**, 3174-74-1; **8**, 19611-45-1; **9**, 77342-93-9; **12**, 143192-19-2; **13**, 143215-11-6; **14**, 143215-12-7; **15**, 143192-20-5; TPP, 1162-70-5; $[Rh_2(\mu\text{-}Cl)_2(cod)_2]$, 12092-47-6; PPh_3, 603-35-0; $P(OPh)_3$, 101-02-0; $P(OMe)_3$, 121-45-9; $P(OPh^*)_3$, 31502-36-0; dimethyl(3-mercaptopropyl)amine, 42302-17-0.

Supplementary Material Available: Table S1, a complete set of distances and angles, Table S2, thermal parameters for all non-hydrogen atoms, and Table S3, hydrogen atom positional parameters (7 pages). Ordering information is given on any current masthead page.

OM920094O

(32) Walker, N.; Stuart, D. *Acta Crystallogr., Sect. A* **1983**, *A39*, 158.
(33) Cromer, D. T.; Waber, J. T. *Acta Crystallogr.* **1965**, *18*, 104.